*J. Fluid Mech.* (1986), *vol.* 163, *pp.* 393–403
*Printed in Great Britain*



# Anisotropy of the temperature dissipation in a turbulent wake

By R. A. ANTONIA AND L. W. B. BROWNE
Department of Mechanical Engineering, University of Newcastle, N.S.W. 2308, Australia

(Received 15 May 1985 and in revised form 20 August 1985)

Measurements by Freymuth & Uberoi (1971) of the terms in the transport equation for the temperature variance in a plane turbulent wake indicated approximate equality for the three components of the temperature dissipation, thus indicating isotropy for that quantity. This result was in sufficient disagreement with the results obtained in several other turbulent shear flows to warrant further measurements of the temperature dissipation in the wake. The present measurements indicate that the dissipation is larger than the isotropic value by about 50 % near the wake centreline and nearly 100 % near the region of maximum production. The magnitude of this ratio is similar to that obtained in other turbulent shear flows. The present measured ratio of total dissipation to isotropic dissipation leads to a satisfactory closure of the temperature variance budget for our experiments and also for the plane-wake measurements of Fabris (1974). It is concluded that the temperature dissipation is not isotropic.

## 1. Introduction

The transport equation for $\frac{1}{2}\overline{\theta^2}$ ($\theta$ is the temperature fluctuation) in a plane wake can be approximated to (e.g. Freymuth & Uberoi 1971, hereinafter referred to as I)

$$\tfrac{1}{2}U_1\frac{\partial\overline{\theta^2}}{\partial x}+\overline{v\theta}\frac{\partial \overline{T}}{\partial y}+\frac{1}{2}\frac{\partial}{\partial y}\overline{v\theta^2}+N=0. \tag{1}$$

$U_1$ is the free-stream velocity, $\overline{T}$ is the mean temperature relative to ambient, $v$ is the velocity fluctuation in the lateral $y$-direction (the coordinate system is shown in the inset of figure 1), while $N$ is the average temperature dissipation defined as

$$N=\alpha\left(\overline{\left(\frac{\partial\theta}{\partial x}\right)^2}+\overline{\left(\frac{\partial\theta}{\partial y}\right)^2}+\overline{\left(\frac{\partial\theta}{\partial z}\right)^2}\right), \tag{2}$$

where $\alpha$ is the thermal diffusivity.

An important experimental result obtained in I, where all the terms in (1) were measured in the self-preserving region of the wake, was that the three components of $N$ were approximately equal, indicating support for local isotropy. In this case $N$ is equal to its isotropic value $N_i$,

$$N_i=3\alpha\overline{\left(\frac{\partial\theta}{\partial x}\right)^2}. \tag{3}$$

The correctness of (3) seemed enhanced by the fact that relation (1) was reasonably satisfied by the measurements. Further, Freymuth & Uberoi (1973) assumed relation (3) and also obtained a reasonable closure for (1) in the self-preserving region of the wake of a sphere.

There have now been several attempts to determine the three components of $N$ in different shear flows. Defining $K_1 = \overline{(\partial\theta/\partial y)^2}/\overline{(\partial\theta/\partial x)^2}$ and $K_2 = \overline{(\partial\theta/\partial z)^2}/\overline{(\partial\theta/\partial x)^2}$, Sreenivasan, Antonia & Danh (1977) found, in the log region of a turbulent boundary layer, average values of $K_1$ and $K_2$ equal to about 1.19 and 1.46 respectively. Verollet's (1972) measurements in the inner region of a turbulent boundary layer indicated values of $K_1$ and $K_2$ that increased from about unity near the edge of the log region to about 2.39 and 2.04 respectively closer to the wall. Tavoularis & Corrsin (1981) considered a quasi-homogeneous turbulent shear flow with a constant temperature gradient and obtained $K_1 \approx K_2 \approx 1.83$. A similar result was obtained by Antonia, Brown & Chambers (1983) in the self-preserving region of a turbulent plane jet, with $K_1 \approx K_2 \approx 1.5$ at the centreline. The above results, although in disagreement with (3), also gave adequate closures of the budgets of $\frac{1}{2}\overline{\theta^2}$ in the various flows. It was clear then that re-evaluation and re-measurement of the dissipation terms in the plane wake were warranted.

In all the cited investigations, $\partial\theta/\partial x$ was evaluated using Taylor's hypothesis, namely

$$\frac{\partial\theta}{\partial x} = -\frac{1}{\overline{U}}\frac{\partial\theta}{\partial t}, \tag{4}$$

where $\overline{U}$ is the mean velocity in the $x$-direction. A recent direct experimental confirmation of (4) in a plane jet by Browne, Antonia & Rajagopalan (1983) suggests that this assumption should be adequate in general. A more likely cause of difficulty is the measurement of the spatial derivatives $\partial\theta/\partial y$ and $\partial\theta/\partial z$. With the exception of Verollet's (1972) measurements, which were made using the correlation approach, these derivatives have been obtained by forming the difference $\Delta\theta$ between temperature signals from a pair of parallel cold wires. There are several errors associated with the use of such an arrangement (e.g. Mestayer & Chambaud 1979; Tavoularis & Corrsin 1981; Browne, Antonia & Chambers 1983; Browne, Antonia & Rajagopalan 1983), the most important error being the experimental uncertainties in static calibrations of the wires for small wire separations. There is also a need to extrapolate distributions of $\overline{(\Delta\theta/\Delta y)^2}$ and $\overline{(\Delta\theta/\Delta z)^2}$ to determine their 'correct' values. Since only one separation was used in I, it is possible that the results presented for $\overline{(\partial\theta/\partial y)^2}$ and $\overline{(\partial\theta/\partial z)^2}$ are incorrect.

In the present investigation, the budget of $\frac{1}{2}\overline{\theta^2}$ is determined in the self-preserving region of a two-dimensional turbulent wake, with special attention being paid to the measurement of dissipation. Experimental conditions, described in §2, were designed to be similar to those of I. Experimental results are discussed in §3 in the context of those of I. Detailed measurements of turbulence quantities in a two-dimensional turbulent wake have been published by Fabris (1974, 1979*a*, *b*). These measurements enabled the calculation of all the terms in (1) except $N$, since only $\overline{(\partial\theta/\partial x)^2}$ was obtained. Results for Fabris' budget are also presented in §3.

## 2. Experimental arrangement and conditions

Experiments were carried out in a non-return blower-type wind tunnel with a $350 \times 350$ mm working section, 2.4 m long. Two-dimensionality of the flow and the absence of longitudinal vortices in the working section were established and checked prior to these experiments. Also the floor of the working section was slightly tilted (by 20 mm in 2.4 m) to maintain a zero presure gradient, the maximum variation in static pressure being 0.1 % of the dynamic pressure.

| | Present experiments | Experiments of Freymuth & Uberoi (1971) | Experiments of Fabris (1974) |
|---|---|---|---|
| Cylinder diameter, $d$ mm | 2.67 | 2.8 | 6.26 |
| Free-stream velocity, $U_1$ m/s | 6.70 | 6.10 | 6.46 |
| Reynolds number, based on $d$, $R_d = U_1 d/\nu$ | 1170 | 950 | $\simeq 2700$ |
| Centreline values at position of detailed measurements: | | | |
| Location, $x/d$ | 420 | 1140 | 400 |
| Kolmogorov microscale, $L_K$ mm | 0.45 | 0.9 | 0.66 |
| Taylor microscale, $\lambda$ mm | 5.2 | 9.9 | 10.5 |
| $\overline{u^2}^{\frac{1}{2}}/U_1$ (%) | 1.6 | 0.92 | 1.47 |
| Reynolds number based on Taylor microscale (independent of $x$) $R_\lambda = \lambda \overline{u^2}^{\frac{1}{2}}/\nu$ | 36 | 31 | 67 |
| Mean-velocity defect, $U_0$ m/s | 0.36 | 0.21 | 0.367 |
| Mean-temperature excess, $T_0$ °C | 0.82 | 1.14 | 0.34 |
| Mean-velocity defect half-width, $L$ mm | 12.3 | 20.3 | 30.5 |

TABLE 1. Summary of experimental conditions

The wake-generating body was a stainless-steel tube of 2.67 mm outer diameter mounted horizontally in the mid-plane of the working section and 20 cm after the start of the working section. Electric heating of 100 W provided temperature as a passive marker of the flow in the self-preserving region. Details of the experimental conditions for these experiments and for those of I and Fabris (1974) are contained in table 1. The difference (table 1) in the values of $\lambda$, $L_K$, $U_0$, $T_0$, $L$ between the present experiment and I reflect differences in the heating conditions and measurement locations. In I, a heating input of 250 W was used and measurements were made at $x/d = 1140$. For the present experiment a smaller amount of heating seemed preferable, and, to maintain a satisfactory signal-to-noise ratio for the temperature fluctuation, a smaller value of $x/d$ was then necessary. The choice of 420 for $x/d$ appeared to be a reasonable compromise; our experiments indicated approximate self-preservation from $x/d \approx 200$, although the experiments of LaRue & Libby (1974) indicated that self-preservation is only achieved at $x/d \approx 400$.

Velocity fluctuations and mean values were measured using 5 μm diameter Pt–10% Rh hot wires, 0.9 mm long, with DISA 55M anemometers. As appropriate, a single wire was used for $u$ (the velocity fluctuation in the longitudinal $x$-direction) while an X-wire, with wires separated by about 0.9 mm, was used in the $(x, y)$-plane for $u$ and $v$ and in the $(x, z)$-plane for $u$ and $w$. For measurements of the longitudinal velocity derivative, required for the determination of $\lambda$ and $L_K$, a single wire (2.5 μm Pt) of length 0.4 mm was used.

Temperature measurements were made using 0.63 μm dimeter Pt–10% Rh cold wires operated with in-house constant-current anemometers supplying 0.1 mA. Wire lengths in the range 0.4–1 mm were used for correlation and derivative measurements. For the measurements of $\overline{v\theta}$, a cold wire was located about 0.5 mm in front of the wire-crossing point of an X-probe. To avoid any possible interference of the unetched wire stubs with the X-probe, a 1 mm long cold wire was used. For the two-point temperature-correlation measurements, two cold wires, mounted on different probes, were located in the same $(y, z)$-plane parallel to each other and to the $z$-axis. Their separation in the $y$- and $z$-directions was controlled by traversing mechanisms with a least count of 0.01 mm. Initial separations were measured, using a theodolite, with an accuracy estimated at $\pm 0.02$ mm.

After appropriate gain and offset all fluctuating signals were filtered ($f_c = 2000$ Hz) and sampled ($f_s = 4000$ Hz) directly into a computer using an 11-bit plus-sign A/D converter. All processing was done on the same computer using constants carefully obtained from velocity, temperature and yaw calibrations. Mean quantities from the anemometers were determined using a small data-logging system operating at a sampling frequency of 10 Hz.

## 3. Results and discussion

The production, diffusion and dissipation terms in (1) were obtained directly from measured quantities. Use was made of self-preservation to calculate the advection term. The self-preserving form for $\overline{\theta^2}$ is given by

$$\overline{\theta^2} = T_0^2 h(\eta),$$

where $T_0$ is the centreline value of $\overline{T}$ and $\eta = y/L$, $L$ being the value of $y$ where the velocity defect is half its centreline value $U_0$. The gradient $\partial\overline{\theta^2}/\partial x$ can then be inferred from the streamwise variations of $T_0$, $L$ and from the distributions of $h$ and its derivative $h'$.

Mean and r.m.s. velocity and temperature profiles measured in the range $100 \leqslant x/d \leqslant 600$ indicated that self-preservation was satisfied approximately for $x/d \gtrsim 200$. The centreline variations of $L$, $U_0$ and $T_0$ for $x/d \gtrsim 200$ were given approximately by

$$\frac{L}{d} = 0.20\left(\frac{x}{d}+125\right)^{\frac{1}{2}}, \tag{5}$$

$$\frac{U_0}{U_1} = 1.28\left(\frac{x}{d}+125\right)^{-\frac{1}{2}} \tag{6}$$

and

$$\frac{T_0}{T_{\text{ref}}} = 23.34\left(\frac{x}{d}+125\right)^{-\frac{1}{2}}. \tag{7}$$

For convenience, the reference temperature $T_{\text{ref}}$, relative to ambient, is identified with the value of $T_0$ at $x/d = 420$. Relations (5) and (6) yield values of $4.27 \times 10^{-3}$ and 0.054 for $\mathrm{d}L/\mathrm{d}x$ and $U_0/U_1$ at $x/d = 420$, justifying the 'thin shear layer' and 'small velocity defect' approximations which have been made in obtaining (1). There was no discernible departure from zero for the correlations $\overline{uw}$ and $\overline{w\theta}$ ($w$ is the velocity fluctuation in the $z$-direction) at any location in the wake, consistent with the approximation of two-dimensionality in (1).

The distributions of $h$, $\overline{T}$, $\overline{v\theta}$, $\overline{v\theta^2}$ were obtained by applying cubic-spline least-squares fits to experimental values. For the derivatives $h'$, $\partial\overline{T}/\partial y$ and $\partial\overline{v\theta^2}/\partial y$, the least-squares fits to $h$, $\overline{T}$ and $\overline{v\theta^2}$ were differentiated numerically, and further least-squares fits were applied to the derivative data. Self-preserving forms for $(U_1-\overline{U})/U_0$, $\overline{U}$ being the mean velocity in the $x$-direction, and $\overline{T}/T_0$ are shown in figure 1. Self-preserving forms for $\overline{\theta^2}^{\frac{1}{2}}/T_0$ and $\overline{v\theta}/U_0T_0$ are presented in figures 2 and 3 respectively. The present distributions of $(U_1-\overline{U})/U_0$, $\overline{T}/T_0$, $\overline{\theta^2}^{\frac{1}{2}}/T_0$ and $\overline{v\theta}/U_0T_0$ are in closer agreement with those of Fabris (1974) than of I. The distribution of $\overline{v\theta}/U_0T_0$, calculated from the mean-enthalpy equation using approximate self-preservation and the relations (5), (6), (7), is in reasonable agreement with the present measured distribution of $\overline{v\theta}/U_0T_0$

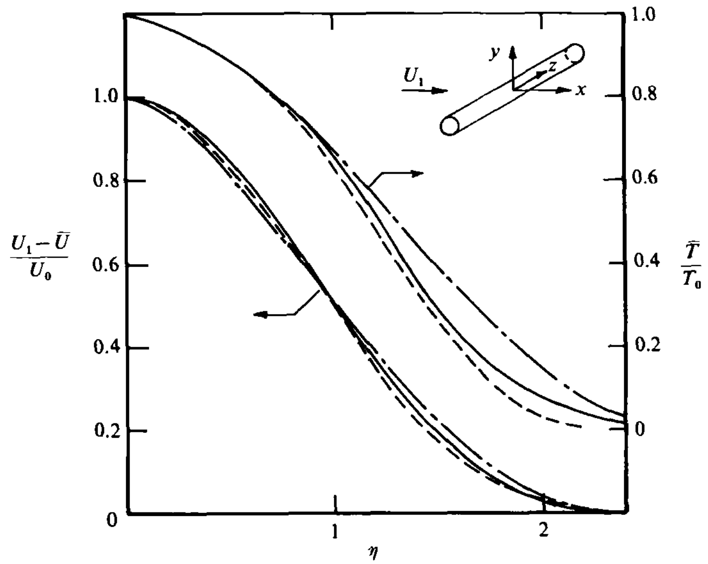


FIGURE 1. The coordinate system and mean-velocity defect and mean-temperature-excess profiles in self-preserving coordinates. ——, present; — - —, I; — —, Fabris (1974).

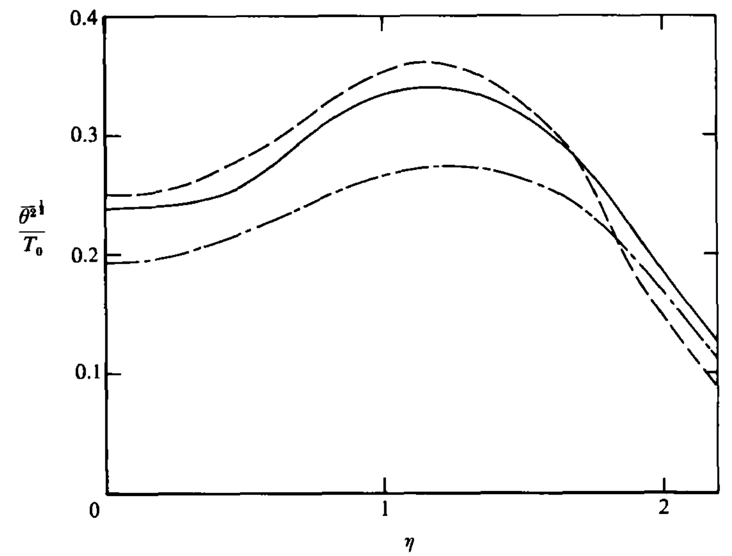


FIGURE 2. Distributions of root-mean-square temperature $\overline{\theta^2}^{\frac{1}{2}}/T_0$. ——, present; — - —, I; — —, Fabris (1974).

(the uncertainty of this measurement was estimated to be about $\pm 12\%$). At $\eta = 1$, the measured distribution is smaller than the calculation by about 10 %. In contrast, measured and calculated distributions reported in I indicated that, at $\eta \simeq 1$, the calculation was larger than measurement by about 35 %. Since information analogous to (5), (6), (7) was not available, a calculation of $\overline{v\theta}$ relevant to Fabris' experimental conditions was not made.

The component $\alpha\overline{(\partial\theta/\partial x)^2}$ of the dissipation $N$ was obtained from measurements

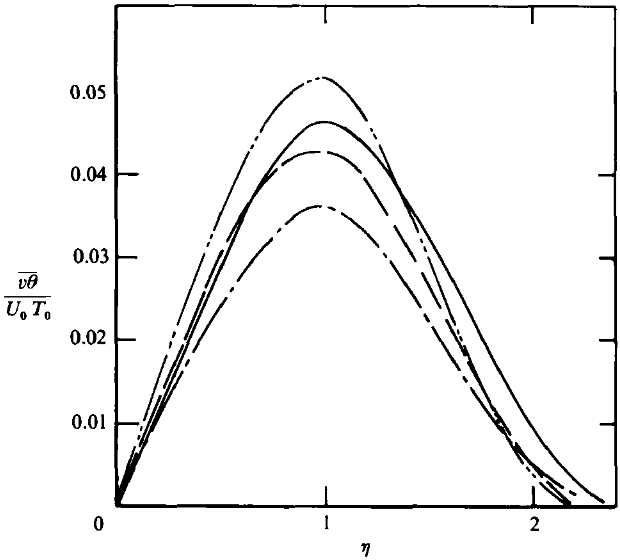


FIGURE 3. Distributions of lateral heat flux $\overline{v\theta}/U_0 T_0$. —, present; — - —, I; — —, Fabris (1974); — - - —, calculation using the mean-enthalpy equation, self-preservation and relations (5), (6), (7).

of $\overline{(\partial\theta/\partial t)^2}$ using one cold wire and Taylor's hypothesis, (4). The other two components, which involve gradients $\partial\theta/\partial y$ and $\partial\theta/\partial z$, were estimated from the behaviour of temperature autocorrelations for small separations of two cold wires in the $y$- or $z$-directions. The autocorrelation function $\rho_\beta$ is defined by

$$\rho_\beta(\Delta\beta, \tau) = \frac{\overline{\theta(\beta, t)\,\theta(\beta+\Delta\beta, t+\tau)}}{\overline{\theta^2(\beta)}^{\frac{1}{2}}\,\overline{\theta^2(\beta+\Delta\beta)}^{\frac{1}{2}}},$$

where $\tau$ is the time delay and $\beta$ stands for either $x$, $y$ or $z$. With the assumption of homogeneity, the limiting behaviour of $\rho_\beta$ at $\tau = 0$ and small values of $\Delta\beta$ can be approximated (e.g. Batchelor 1953), to order $(\Delta\beta)^4$, by

$$\rho_\beta(\Delta\beta, 0) \simeq 1 - \frac{\overline{(\Delta\beta)^2}}{2\lambda_\beta^2}, \tag{8}$$

where $\lambda_\beta$ is the temperature Taylor microscale, defined as

$$\lambda_\beta^2 = \frac{\overline{\theta^2}}{\overline{\left(\frac{\partial\theta}{\partial\beta}\right)^2}}. \tag{9}$$

Using (8), the relative magnitudes of the Taylor microscales, and thus the relative magnitudes of the dissipation components $\overline{(\partial\theta/\partial\beta)^2}$, can be estimated from the curvatures of the $\rho_\beta$ *versus* $\Delta\beta$ curves near the origin. Distributions of $\rho_\beta$, for relatively small values of $\Delta\beta$, are shown in figure 4, at two values of $\eta$. The curvatures of the $\rho_\beta$ distributions in figure 4 indicate that $K_2 > K_1$. This inequality, more marked for $\eta \simeq 1.8$ than $\eta = 0$, contrasts with the approximate equality of the three mean-square derivatives found in I.

The magnitude of $\lambda_x$ was obtained from measurements of $\overline{\theta^2}$ and $\overline{(\partial\theta/\partial x)^2}$. To determine the appropriate magnitude of $\lambda_\beta$, $\beta = y$ or $z$, (8) was used to calculate $\lambda_\beta$ for each separation $\Delta\beta$. This calculation shows that there is a small range of $\Delta\beta$ over

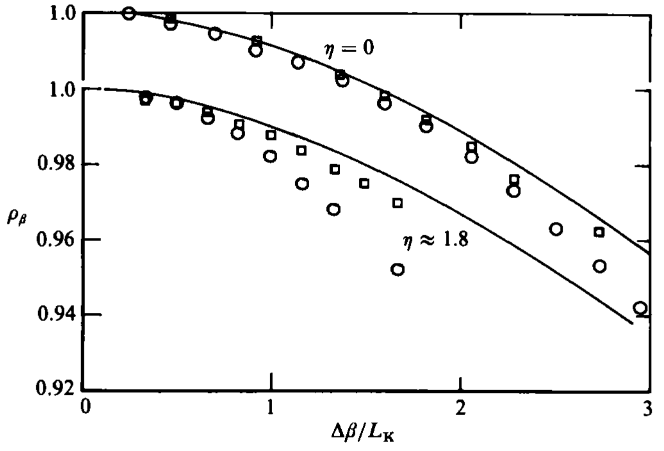


FIGURE 4. Spatial correlations of temperature at $\eta = 0$ and $\eta \approx 1.8$ ($x/d = 420$). $\Delta\beta$ is the wire separation and $L_K$ the Kolmogorov microscale. —, $\beta = x$; ○, $y$; □, $z$.

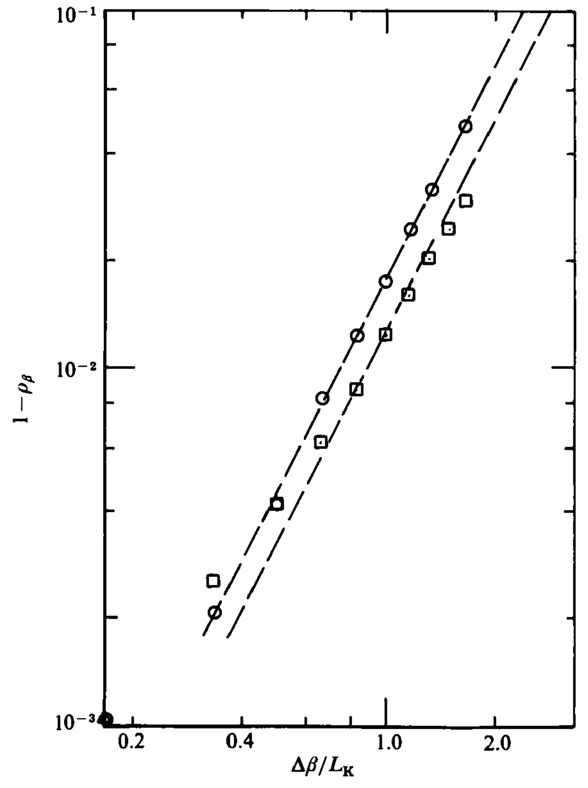


FIGURE 5. Log–log representation of $(1-\rho_\beta)$ as a function of $\Delta\beta/L_K$ at $\eta = 1.8$ ($x/d = 420$). ○, $\beta = y$; □, $z$.

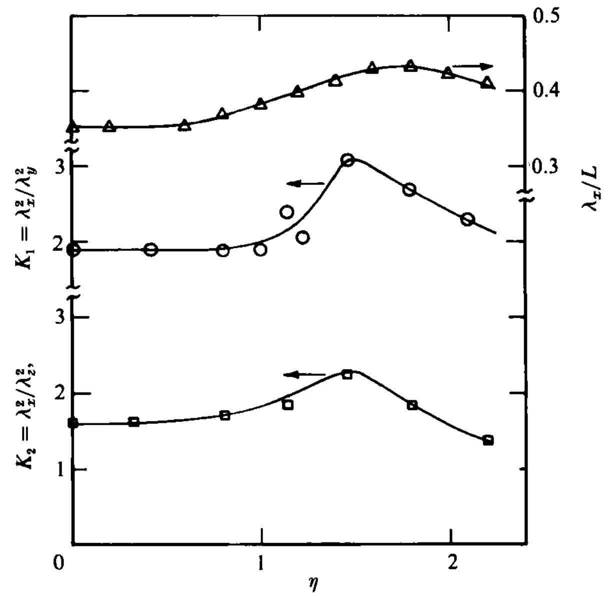


FIGURE 6. Distributions of $\lambda_x/L$ and of the ratios $K_1$ and $K_2$ at $x/d = 420$.

which $\lambda_\beta$ is approximately constant; the equivalent geometrical determination of $\lambda_\beta$ consists of plotting $(1-\rho_\beta)$ *versus* $\Delta\beta$ on a log–log plot and identifying the extent of the data, which exhibit a slope of $+2$. Such a construction, shown in figure 5 for $\eta \simeq 1.8$, indicates a small range of $\Delta\beta/L_K$ which satisfies the parabolic behaviour of (8). The particular values for $\lambda_y$ and $\lambda_z$ inferred from figure 2 are equal to about 3.24 mm and 3.87 mm respectively. For comparison, the magnitude of $\lambda_x$ is equal to about 5.30 mm. The departure of the data from the expected slope for very small values of $(1-\rho_\beta)$ was also observed in other flows (e.g. the temperature data of Antonia *et al.* 1984, and the velocity data of Rose 1966 and Lawn 1971). Sources of inaccuracy at small separations have been discussed by Antonia *et al.* (1984), but it should also be noted that, apart from the uncertainty in determining $\Delta\beta$, the expected maximum of unity for $\rho_\beta$ is not quite achieved in practice in view of the inevitable contamination by electronic noise. Signal-to-noise ratios, on an r.m.s. basis, for the present measurements were typically equal to about 10. Such noise contamination reduced the maximum measured value of $\rho_\beta$ to about 0.95; correcting the measured correlation for the noise in each of the two measuring circuits and for any correlation between the noise components in the different circuits, restored the maximum value of $\rho_\beta$ to almost 1.0. The possibility of error, due to the assumed homogeneity in (8), was checked at $\eta \simeq 1$ where the mean velocity gradient is largest. The coefficient $\rho_y$ was measured for both positive and negative values of $\Delta y$ but the distribution of $\rho_y$ *versus* $|\Delta y|$ remained unchanged, so that $\lambda_y$ was unaffected. Similarly, we found that, independently of $\eta$, $\lambda_z$ was independent of the direction of $\Delta z$, an observation which supports the assumed two-dimensionality of the mean flow.

The ratio of $\lambda_x/L$, plotted in figure 6, is approximately constant near the wake centreline but increases to a maximum near $\eta = 1.8$. It should be noted that, although a correction due to electronic noise was applied to the $\overline{(\partial\theta/\partial x)^2}$ measurements, no wire-length correction was made, since the wire length was comparable with or smaller than the Kolmogorov microscale. Using the values of $\lambda_x$ shown in figure 6

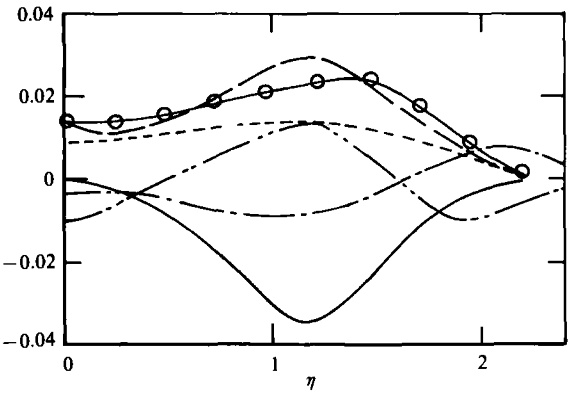


FIGURE 7. Budget of $\frac{1}{2}\overline{\theta^2}$ at $x/d = 420$. All terms are normalized. ——, production; — - - —, diffusion; — — —, advection; – – –, isotropic dissipation; $\ominus$, total measured dissipation; — —, dissipation required for closure.

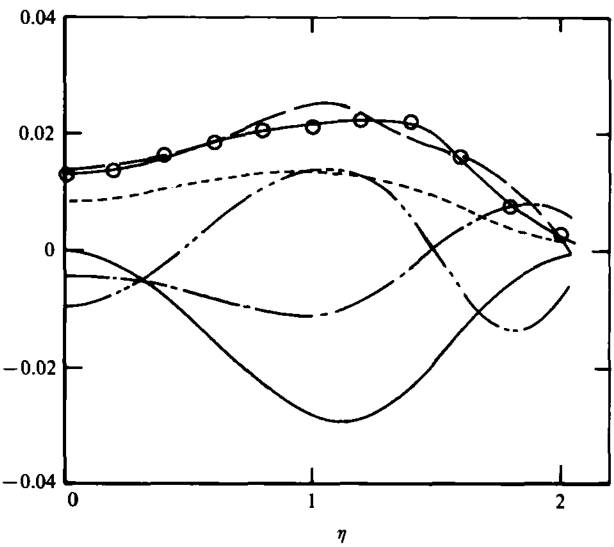


FIGURE 8. Budget of $\frac{1}{2}\overline{\theta^2}$ calculated using the data of Fabris (1974) at $x/d = 420$. ——, production; — - - —, diffusion; — — —, advection; – – –, isotropic dissipation; $\ominus$, total dissipation obtained by using the present distribution of $N/N_1$; — —, dissipation required for closure.

and the values of $\lambda_y$ and $\lambda_z$ inferred from the spatial-correlations procedure, distributions of $\lambda_x^2/\lambda_y^2$, i.e. $K_1$, and $\lambda_x^2/\lambda_z^2$, i.e. $K_2$, are also plotted in figure 6. These ratios are relatively constant near $\eta = 0$ but their magnitudes are significantly larger than the locally isotropic value of unity. For $\eta > 1$, the departure from isotropy increases further, especially for $K_1$, and is largest near $\eta = 1.5$.

All terms in (1) are plotted in figure 7 after normalization by $L/U_0 T_0^2$. The qualitative behaviour of each of the terms is in agreement with that of the corresponding terms in the budget presented in I and also in the budget (figure 8) calculated using the data of Fabris (1974, 1979*a*). The significant point of difference is the ratio of the total-to-isotropic dissipation, which for the present budget is about 1.5 near the centreline and reaches a maximum of about 2.0 near $\eta = 1.4$. In contrast,

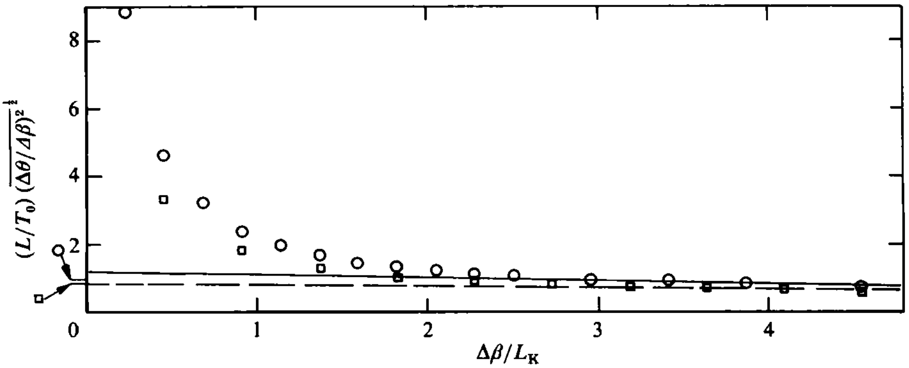


FIGURE 9. Dependence of r.m.s. temperature differences on the normalized separation $\Delta y/L_K$ or $\Delta z/L_K$. ○, $\beta = y$; □, $\beta = z$; ——, linear extrapolation of data for $\Delta y/L_K \gtrsim 3$; — —, linear extrapolation of data for $\Delta z/L_K \gtrsim 3$. Arrows indicate values obtained from correlation method.

I indicated a value of unity, almost independently of $\eta$. For the present budget, the overall imbalance (the dissipation required for closure is shown in figures 7 and 8) is negligible near the wake centreline ($\eta \lesssim 0.8$) and remains satisfactorily small in the region of $\eta > 0.8$. It is of interest to note in figures 7 and 8 that the diffusion is more important than the advection at the wake centreline and is slightly larger than the advection at the location where the production (and also dissipation) is largest. The discrepancy between $N$ and $N_1$ is also largest at this location. The plausibility of the present values of $N/N_1$ is further demonstrated in figure 8; it is clear from this figure that the isotropic dissipation measured by Fabris (1974) is insufficient to enable closure of the budget. When the present values of the ratio $N/N_1$ are applied to Fabris' isotropic dissipation, the resulting dissipation distribution agrees reasonably well with that required for closure.

It is difficult to provide an explanation for I's corroboration of isotropy in the context of the three components of $N$ and the success of I in closing the budget. This success is especially puzzling in view of the technique used by these authors to determine the derivatives with respect to $y$ and $z$; as noted earlier, the separation between the wires was fixed and the derivatives calculated using differences $\Delta\theta/\Delta y$ and $\Delta\theta/\Delta z$. We estimate that this wire separation, at $\eta = 0$, was equal to about $0.9L_K$. Our measured distributions, figure 9, of $\overline{(\Delta\theta/\Delta y)^2}^{\frac{1}{2}}$ *versus* $\Delta y/L_K$ and $\overline{(\Delta\theta/\Delta z)^2}^{\frac{1}{2}}$ *versus* $\Delta z/L_K$ indicate that, for this separation, the measured r.m.s. values are larger than the values obtained using the correlation technique by factors of about 2.6 and 2.2 respectively, thus further increasing the anisotropy.

A linear extrapolation to zero separation of the data for which $\Delta x$ and $\Delta y$ are both larger than $3L_K$, as shown in figure 9, gives satisfactory agreement, within the uncertainty of the extrapolation, between the extrapolated values and those determined by the correlation method. There is, however, no rigorous justification for such an extrapolation. In view of the theoretical basis of the correlation approach, we have preferred to adopt the correlation method in the present paper.

## 4. Concluding remarks

Although the qualitative form of each of the terms in the present budget of $\frac{1}{2}\overline{\theta^2}$ is similar to that presented by I, the present measurements do not corroborate those authors' observation that the three components of dissipation satisfy isotropy. Mean-square values of transverse derivatives of temperature are larger than those for the longitudinal derivative, the total dissipation being larger than the isotropic dissipation by an amount varying from 50 % near the centreline to almost 100 % near the wake half-width. The measured total dissipation yields a satisfactory closure of the budget for $\frac{1}{2}\overline{\theta^2}$. When the present measured ratio of total-to-isotropic dissipation is applied to the isotropic-dissipation measurements of Fabris (1974), a satisfactory closure is also obtained for the $\frac{1}{2}\overline{\theta^2}$ budget calculated using Fabris' data.

The anisotropy of the temperature dissipation appears to be a universal feature of sheared scalar fields and seems independent of the Reynolds number. It is important that this non-equality be taken into account in models of turbulent heat transfer. It should, however, be emphasized that equality between the mean-square values of first-order temperature derivatives represents only one test for isotropy. Antonia & Browne (1983), from measurements in a turbulent plane jet, pointed out that second-order temperature derivatives provide a more sensitive test of isotropy of the very fine-scale fluctuations than first-order derivatives.

The support of the Australian Research Grants Scheme is appreciated. The authors are grateful to Dr A. J. Chambers for his contribution to the design of the wake facility and to Mr C. S. Teo for his assistance in checking the quality of the flow.

## REFERENCES

Antonia, R. A. & Browne, L. W. B. 1983 *J. Fluid Mech.* **134**, 67.

Antonia, R. A., Browne, L. W. B., Britz, D. H. & Chambers, A. J. 1984 *Phys. Fluids* **27**, 87.

Antonia, R. A., Browne, L. W. B., Chambers, A. J. & Rajagopalan, S. 1983 *Intl J. Heat Mass Transfer* **26**, 41.

Batchelor, G. K. 1953 *Theory of Homogeneous Turbulence*. Cambridge University Press.

Browne, L. W. B., Antonia, R. A. & Chambers, A. J. 1983 *Boundary-Layer Met.* **27**, 129.

Browne, L. W. B., Antonia, R. A. & Rajagopalan, S. 1983 *Phys. Fluids* **26**, 1222.

Fabris, G. 1974 Ph.D. thesis, Illinois Institute of Technology.

Fabris, G. 1979*a* *Turbulent Shear flows*, vol. I (eds. F. Durst, B. E. Launder, F. W. Schmidt & J. H. Whitelaw), p. 55. Springer.

Fabris, G. 1979*b* *J. Fluid Mech.* **94**, 673.

Freymuth, P. & Uberoi, M. S. 1971 *Phys. Fluids* **14**, 2574.

Freymuth, P. & Uberoi, M. S. 1973 *Phys. Fluids* **16**, 161.

LaRue, J. C. & Libby, P. A. 1974 *Phys. Fluids* **17**, 873.

Lawn, C. J. 1971 *J. Fluid Mech.* **48**, 477.

Mestayer, P. & Chambaud, P. 1979 *Boundary-Layer Met.* **16**, 311.

Rose, W. G. 1966 *J. Fluid Mech.* **25**, 97.

Sreenivasan, K. R., Antonia, R. A. & Danh, H. Q. 1977 *Phys. Fluids* **20**, 1238.

Tavoularis, S. & Corrsin, S. 1981 *J. Fluid Mech.* **104**, 349.

Verollet, E. 1972 Ph.D. thesis, Université d'Aix-Marseille II (also *Rapport* CEA-R-4872, C.E.N., Saclay, 1977).